Discrete Covalent Organic−Inorganic Hybrids: Terpyridine Functionalized Polyoxometalates Obtained by a Modular Strategy and Their Metal Complexation

Marie-Pierre Santoni,[†,‡] Amlan K. Pal,[†] Garry S. Hanan,*,[†] Anna Proust,[‡,§] and Bernold Hasenknopf*,[‡]

[†]Department of Chemistry, Université de Montréal, Montréal, Québec H3T-1J4, Canada

[‡]Institut Parisien de Chimie Moléculaire (CNRS UMR 7201), Université Pierre et Marie Curie (UPMC) - Paris 06, Case Courrier 42, 4 place Jussieu, 75005 Paris, France

[§]Institut Universitaire de France, 103 Bd Saint-Michel, 75005 Paris, France

Ⓢ Supporting Information

ABSTRACT: The rational design and synthesis of organic−inorganic hybrids as functional molecular materials relies on both the careful conception of building-blocks and the strategy for their assembly. Three families of trialkoxo polyoxometalates (Lindqvist **2**, Anderson **3**, Dawson **4**) grafted with remote terpyridine coordination sites have been synthesized to extend the available building-blocks. These new units can be combined with metal complexes that play a role as (i) chromophores toward charge-separated systems in light-harvesting devices and (ii) coordination motifs for metal-directed self-assembly toward multifunctional molecular hybrid materials. The X-ray crystal structures of polyoxometalate-terpyridine hybrids indicate distances of 21 Å and 19 Å between the two terpyridyl coordination sites in **2** and **3**, respectively, with angles between the coordination vectors of 180° and 177.4°, respectively. Lindqvist **2** displays a reduction at −0.52 V vs SCE while Anderson **3** exhibits one reversible oxidation attributed to Mn(III)/Mn(IV) (+0.75 V vs SCE) and a broad wave at −1.28 V vs SCE assigned to the Mn(III)/Mn(II) reduction. Dawson **4** displays several processes on a wide range of potentials (+0.5 to −2.0 V vs SCE) centered on V(V), W(VI) and the organic ligand in order of decreasing potentials. The grafted terpyridine ligands in Anderson **3** and Dawson **4** were successfully coordinated to {PdCl}$^+$ and {RuCl$_3$} moieties, respectively. The polyoxometalates and transition metal complexes retain their intrinsic properties in the final assemblies.
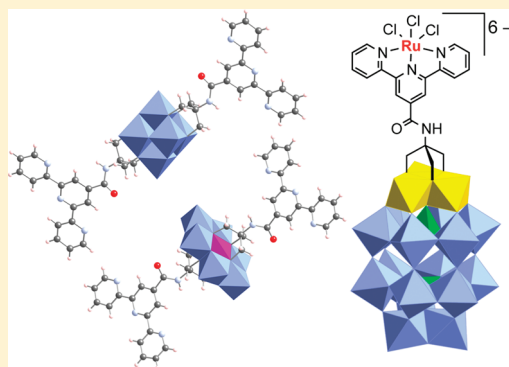
■ INTRODUCTION

New developments in hybrid materials are driven by current technological challenges, such as solar energy conversion. The interest in hybrid systems stems from the retention of their intrinsic properties in multicomponent assemblies. Thus, the properties of hybrid materials can be optimized for a given targeted application based on the individual components used in the final material.[1] In this respect, inorganic building blocks such as polyoxometalates[2] (POMs) are interesting components as they present various properties such as redox activity,[3] photochromism,[4] and magnetism.[4,5] They have been extensively combined with organic donors[6] and transition metal complexes[7] to form hybrid systems toward multifunctional materials. From the point of view of applications in solar energy conversion, POMs are limited to their absorptivity in the UV region,[8] unless they can be photosensitized in the visible part of the solar spectrum by transition metal complexes.[9] The redox-active POMs could then be used either as catalysts,[8] subsequent to charge separation, or they could provide photoaccumulation of charges for catalytic centers in light-harvesting devices.[3] Indeed, fuel production is a multielectronic

process,[10] while light-induced redox reactions are monoelectronic;[11] therefore, a redox mediator is necessary for efficient multielectron storage.

So far, most of the POM-based hybrids found in the literature display functional subunits with *electrostatic* interactions. Coordination of transition metal complexes to the oxo ligands of POMs is common, but control of their position is limited, and the multidimensional networks obtained are often unpredictable.[12] Covalent systems, with organic ligands covalently grafted to the POM framework, are less frequently reported. This disparity is mainly due to the synthetic problems one must overcome to produce a covalent hybrid.[13] For example, multistep synthetic work is usually necessary to achieve organic functionalization of a POM with more elaborate functions.[14] Furthermore, the complexation of metal ions on remote coordination sites, provided by organic ligands grafted on POMs, is challenging because of the competition with coordination sites on the oxo framework.[15,16]

Scheme 1. Strategy for a Modular Assembly of Transition Metal Functionalized POMs (Lindqvist, Anderson, and Dawson)[a]
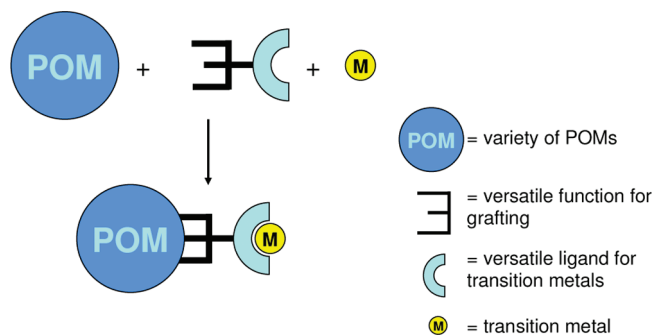

[a] A versatile organic function that can be incorporated into diverse POMs is covalently linked to a versatile terpyridine ligand for transition metal ions.

In addition, the complexation of cationic metal ions on anionic POM-grafted ligands competes with ionic interactions, which leads to the formation of insoluble salts.[17] In spite of these difficulties, interest in covalent molecular systems[18] has been continuously growing for several reasons: (i) the covalent interaction, independent of the media (ionic strength, T, pH), leads to robust systems; (ii) the covalent attachment of units allows one to control their respective ratio in the system; (iii) a more rigid covalent link allows better spatial control over the arrangement of subunits, an important parameter in charge-transfer systems.

As we pointed out earlier,[19] a modular approach allows, by distinct synthetic steps, the matching of a specific ligand to a chosen metal ion, and its connection to a selected POM (Scheme 1). The resulting assembly would then be designed/predictable, and its properties tuned by the individual optimization of the components. Synthetic methodologies to achieve such POM-based hybrids via this strategy require an organic molecule that reacts with several POMs and that can be linked to common transition metal cations. Some examples have been reported, featuring the grafting of ligands with free coordination sites onto a POM framework,[18a,20−22] but results reporting the successful coordination of metals on polypyridine-functionalized POM remain scarce. Peng et al. reported the successful synthesis of POM-based coordination polymers with Fe(II),[15] taking advantage of the quantitative complexation of this relatively labile center (compared to Ru(II)). Hill prepared coordination polymers with pyridine grafted Lindqvist vanadates.[17] Characterization and practical use of these polymers were nonetheless limited by their solubility.

Some of us reported the coordination of pyridyl-functionalized Anderson and Lindqvist structures to metalloporphyrins (M = Ru(II), Zn(II)).[16] These hybrids, among the rare examples of discrete structures, take advantage of the unique vacant coordination site in the axial position of the metalloporphyrin. Despite the encouraging observation of energy transfer from the metalloporphyrin to the POM, monodentate coordination turned out to be too weak, leading to nonfunctional materials. Polydentate coordination to functional metal centers would offer the advantage of stronger bonding using the chelate effect. Recent examples showed the introduction of one and two terpyridine motifs on a POM, through imido[15a] or organo-silyl[14d,21] linkage.

Scheme 2. Synthesis of Terpyridyl-triol 1
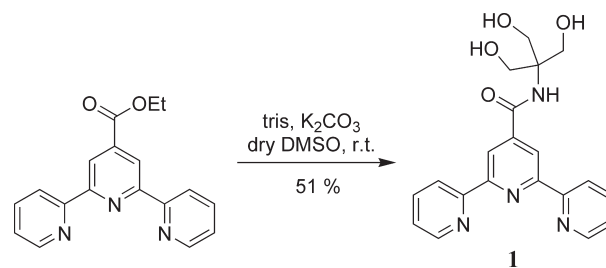
We report here the design of a new polydentate ditopic ligand **1** (Scheme 2), with a triol motif, which connects POM platforms and terpyridyl groups for transition metal binding: POMs **2** (Lindqvist structure), **3** (Anderson structure), and **4** (Dawson structure), each displaying specific redox properties. We also demonstrate that various metals can coordinate to these sites, toward the construction of discrete multifunctional systems with potential as charge-transfer hybrids (for the Ru, **5**) or multicomponent systems (for the Pd, **6**) that could lead to structured assemblies.

■ EXPERIMENTAL SECTION

For Materials and Instrumentation, see the Supporting Information.

Synthesis. $C_{20}H_{20}N_4O_4$, **1**. In a Schlenk flask, tpyCOOEt (1.143 g, 3.7 mmol), $H_2N-C(CH_2OH)_3$ (0.376 g, 3.1 mmol), K_2CO_3 (0.467 g, 3.4 mmol) were suspended in dry dimethylsulfoxide (DMSO, 12 mL) and stirred at room temperature (r.t.) for 15 h under nitrogen atmosphere. The reaction mixture was filtered, and the volume of the brown filtrate was reduced to maximum under vacuum (2 mL left). The remaining brown oil was dissolved in minimum EtOH and precipitated into H_2O (200 mL). The white solid obtained was centrifuged, washed with Et_2O, and dried under vacuum to give pure **1** (0.830 g, 51%). If additional purification is needed, Soxhlet extraction with CH_2Cl_2 can be used. ^1H NMR (d_6-DMSO, 400 MHz, 298 K): δ 8.78 (d, J = 4 Hz, 2H, H_6), 8.75 (s, 2H, $H_{3'}$), 8.66 (d, J = 8 Hz, 2H, H_3), 8.05 (td, J = 8, 2 Hz, 2H, H_4), 7.54 (td, J = 8, 2 Hz, 2H, H_5), 4.75 (t, J = 4 Hz, 3H, H_c), 3.77 (d, J = 8 Hz, 6H, H_b). ESI-MS: $[M+H]^+$ calcd for $C_{20}H_{21}N_4O_4$ 381.1557; found 381.1551. Anal. Calcd for $C_{20}H_{20}N_4O_4$: C, 63.15; H, 5.30; N, 14.73. Found: C, 63.45; H, 5.19; N, 14.25.

$C_{20}H_{20}N_4O$, **1·tBu**. 4'-Carboxyl-2,2′:6′,2′′-terpyridine (tpyCOOH) (0.480 g, 1.7 mmol) was refluxed in $SOCl_2$ (30 mL) for 2.5 h. The yellow clear solution was evaporated to dryness. The residue was suspended in dry dichloromethane (DCM, 12 mL), and a solution of t-butylamine $H_2N-C(CH_3)_3$ (12 mL, 114 mmol) in dry DCM (12 mL) was added dropwise at 0 °C. The brown mixture was left stirring under nitrogen for 15 h. The suspension was poured into water (100 mL) and extracted with DCM to give **1·tBu** (0.435 g, 76%). ^1H NMR (d_6-DMSO, 400 MHz, 298 K): δ 8.78 (d, J = 4 Hz, 2H, H_6), 8.71 (s, 2H, $H_{3'}$), 8.64 (d, J = 8 Hz, 2H, H_3), 8.45 (s, 1H, H_a), 8.04 (td, J = 8, 1 Hz, 2H, H_4), 7.54 (td, J = 8, 2 Hz, 2H, H_5), 1.45 (s, 9H, H_b). $^{13}C\{^1H\}$ NMR (DMSO-d_6, 100 MHz, 298 K): δ 166.5 (CO), 156.7, 156.0, 150.7, 147.0, 138.8, 125.9, 122.2, 119.9, 52.5 (CCH_3), 29.7 (CH_3). UV−vis: λ/nm ($\varepsilon/10^3$ mol^{-1} L cm^{-1}) in CH_3CN, 237 (24.0), 250 (sh), 278 (20.5), 310 (10.1). ESI-MS: $[M+H]^+$ calcd for $C_{20}H_{21}N_4O$ 333.17099; found 333.17177; $[M+Na]^+$ calcd for $C_{20}H_{21}N_4NaO$ 355.15293; found 355.15369. Anal. Calcd for $C_{20}H_{20}N_4O \cdot (H_2O)_{0.25}$: C, 71.30; H, 6.13; N, 16.63. Found: C, 71.13; H, 6.11; N, 16.79. (presence of water confirmed by ^1H NMR)

$(C_{16}H_{36}N)_2[V_6O_{19}(C_{20}H_{17}N_4O)_2]$, **2**. Adapting the published procedure,[16a,17] a Schlenk flask was charged with **1** (0.120 g, 0.16 mmol), $TBA_3H_3[V_{10}O_{28}]$ (0.168 g, 0.05 mmol), and dry DMAc

(4 mL). The orange mixture was heated in the dark at 85 °C for 58 h. The brown solution was filtered on a fine glass frit upon cooling at r.t., and the resulting filtrate was added dropwise to Et_2O (300 mL). The greenish precipitate was centrifuged and reprecipitated twice in a hot mixture of $DMF:CH_3CN:Et_2O$ 2:1:6 (180 mL) to give an orange solid. After recrystallization in DMF/Et_2O, **2** was obtained as orange crystals (76 mg, 37%) suitable for X-ray measurement. ^1H NMR (d_6-DMSO, 400 MHz, 298 K): δ 8.79 (d, J = 4 Hz, 4H, H_6), 8.72 (s, 4H, $H_{3'}$), 8.65 (d, J = 8 Hz, 4H, H_3), 8.46 (s, 2H, H_a), 8.04 (td, J = 8, 2 Hz, 4H, H_3), 7.54 (td, J = 5 Hz, 4H, H_5), 5.36 (s, 12H, H_b), 3.17 (m, 16H, $-NCH_2$-), 1.57 (m, 16H, $-NCH_2CH_2$-), 1.31 (q, J = 10 Hz, 16H, $-NCH_2CH_2CH_2$-), 0.94 (t, J = 8 Hz, 24H, $-NCH_2CH_2CH_2CH_3$). $^{13}C\{^1H\}$ NMR (DMSO-d_6, 175 MHz, 298 K): δ 155.8, 154.9, 149.1, 136.8, 124.0, 120.6, 118.2, 116.9, 81.9 (CCH_2O), 58.0 ($NCH_2CH_2CH_2CH_3$), 23.0 ($NCH_2CH_2CH_2CH_3$), 19.0 ($NCH_2CH_2CH_2CH_3$), 12.5 ($NCH_2CH_2CH_2CH_3$). IR (KBr pellet, cm^{-1}): 2961 (v C−H, m), 2932 (v C−H, m), 2873 (v C−H, m), 1661 (v C=O, vs), 1585 (m), 1538 (s), 1483 (v C−H, m), 1467 (m), 1393 (v C−H, m), 1359 (m), 1310 (m), 1261 (m), 1183 (w), 1150 (w), 1104 (v C−O, s), 1071 (s), 1055 (v C−O, s), 995 (w), 953 (v V=O, vs), 879 (w), 811 (v V−O−V, s), 799 (v V−O−V, s), 765 (w), 719 (v V−O−V, vs), 657 (m), 621 (w), 579 (m), 513 (w). UV−vis: λ /nm (ε /10^3 $mol^{-1} \cdot L \cdot cm^{-1}$) in CH_3CN, 233 (61.1), 248 (57.0), 276 (55.0), 310 (26.7), 350 (7.88). Anal. Calcd for $(C_{16}H_{36}N)_2[V_6O_{19}(C_{20}H_{17}N_4O)_2] \cdot 0.5$ $C_3H_7NO \cdot 2$ H_2O: C, 48.35; H, 6.27; N, 8.05. Found: C, 48.02; H, 6.25; N, 8.37 (presence of disordered solvents confirmed by X-ray diffraction).

$(C_{16}H_{36}N)_3[MnMo_6O_{24}(C_{20}H_{17}N_4O)_2]$, **3**. $(C_{16}H_{36}N)_5$ α−$[Mo_8O_{26}]$ (0.798 g, 0.37 mmol), **1** (0.500 g, 1.31 mmol), and $Mn(CH_3COO)_3 \cdot 2H_2O$ (0.147 g, 0.55 mmol) were suspended in dry DMAc (16 mL). The mixture was heated at 80 °C for 24 h. The reaction mixture was filtered while hot to remove a solid, and the orange filtrate was exposed to Et_2O vapors. Over several hours, an orange crystalline solid forms that is collected to give **3** (0.771 g, 86%). ^1H NMR (d_6-DMSO, 700 MHz, 298 K): δ 64 (br, 12H, H_b), 8.81 (m, 4H, H_6), 8.65 (m, 8H, $H_{3+3'}$), 8.03 (t, J = 7 Hz, 4H, H_4), 7.53 (m, 4H, H_5), 3.16 (m, 24H, $-NCH_2$-), 1.56 (m, 24H, $-NCH_2CH_2$-), 1.30 (q, J = 10 Hz, 24H, $-NCH_2CH_2CH_2$-), 0.93 (t, J = 8 Hz, 36H, $-NCH_2CH_2CH_2CH_3$). $^{13}C\{^1H\}$ NMR (DMSO-d_6, 175 MHz, 298 K): δ 167.8 (CO), 155.6, 155.1, 150.0, 142.0, 138.0, 125.1, 121.3, 119.8, 67.8 (CCH_2O), 57.9 ($NCH_2CH_2CH_2CH_3$), 23.5 ($NCH_2CH_2CH_2CH_3$), 19.7 ($NCH_2CH_2CH_2CH_3$), 14.0 ($NCH_2CH_2CH_2CH_3$). IR (KBr pellet, cm^{-1}): 2961 (v C−H, s), 2936 (v C−H, s), 2873 (v C−H, s), 1690 (m), 1628 (s), 1552 (m), 1480 (v C−H, s), 1394 (s), 1384 (v C−H, s), 1348 (w), 1312 (w), 1263 (w), 1102 (v C−O, m), 1029 (v C−O, s), 941 (v Mo=O, vs), 921 (v Mo=O, vs), 902 (v Mo=O, s), 801 (m), 666 (v Mo−O−Mo, vs), 563 (m). UV−vis: λ/nm (ε/10^3 mol^{-1} L cm^{-1}) in CH_3CN, 233 (148.0), 250 (124.0), 274 (88.5), 312 (36.6). Anal. Calcd for $(C_{16}H_{36}N)_3[MnMo_6O_{26}C_{40}H_{34}N_8] \cdot 0.33$ $C_4H_9NO \cdot 3$ H_2O: C, 43.20; H, 6.13; N, 6.39. Found: C, 42.85; H, 6.14; N, 6.39 (presence of 0.33 equiv. of DMAc and three molecules of water confirmed by ^1H NMR).

$TBA_5H[P_2W_{15}V_3O_{62}(C_{20}H_{17}N_4O)]$, **4**. $(C_{16}H_{36}N)_5[H_4P_2W_{15}V_3O_{62}]$ (314 mg, 0.06 mmol) and **1** (28 mg, 0.07 mmol) were suspended in dry DMAc (0.6 mL). The mixture was heated in the dark at 90 °C for 14 days. The obtained clear orange solution was left to cool down and then poured into Et_2O to precipitate the product. The yellow fine solid was centrifuged, solubilized in minimum acetone (a few drops of EtOH were added), and reprecipitated with Et_2O to give **4** (0.771 g, 86%). ^1H NMR (CD_3CN, 400 MHz, 298 K): δ 8.79 (d, J = 4 Hz, 2H, H_6), 8.74 (s, 4H, $H_{3'}$), 8.69 (d, J = 4 Hz, 2H, H_3), 8.03 (t, J = 7 Hz, 2H, H_4), 7.51 (t, J = 6 Hz, 2H, H_5), 7.09 (s, 1H, H_a), 5.89 (s, 6H, H_b), 3.20 (m, 40H, $-NCH_2$-), 1.67 (m, 40H, $-NCH_2CH_2$-), 1.44 (q, J = 10 Hz, 40H, $-NCH_2CH_2CH_2$-), 1.01 (t, J = 8 Hz, 60H, $-NCH_2CH_2CH_2CH_3$). $^{13}C\{^1H\}$ NMR (CD_3CN, 100 MHz, 298 K): δ 131.5, 129.4, 127.0, 58.8 ($NCH_2CH_2CH_2CH_3$),
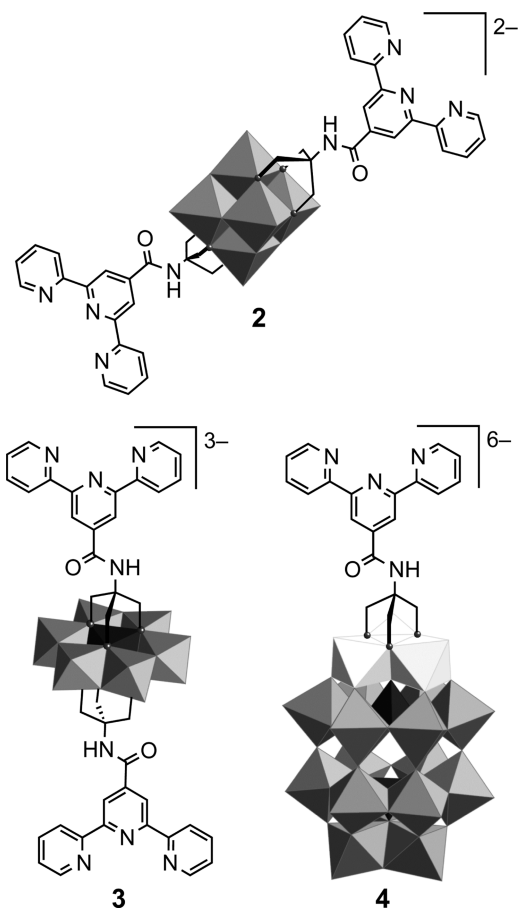
Figure 1. Terpyridine-functionalized POMs **2**−**4**.

37.9 (CCH_2O), 23.9 ($NCH_2CH_2CH_2CH_3$), 22.8, 19.9 ($NCH_2CH_2-CH_2CH_3$), 13.4 ($NCH_2CH_2CH_2CH_3$). ^{31}P NMR (CD_3CN, 162 MHz, 298 K): δ −7.07, −13.16. IR (KBr pellet, cm^{-1}): 2961 (v C−H, s), 2933 (v C−H, s), 2873 (v C−H, s), 1633 (v C=O, m), 1560 (m), 1484 (v C−H, s), 1380 (v C−H, m), 1314 (w), 1261 (w), 1086 (s), 1063 (v C−O, sh), 950 (v M=O, vs), 910 (v M=O, vs), 818 (v M−O−M, vs), 734 (v M−O−M, vs), 528 (m). UV−vis: λ /nm (ε /10^3 $mol^{-1} \cdot L \cdot cm^{-1}$) in CH_3CN, 250 (71.9), 271 (69.9), 307 (38.0). Anal. Calcd for $(C_{16}H_{36}N)_5H[P_2W_{15}V_3O_{63}C_{20}H_{17}N_4]$: C, 21.81; H, 3.62; N, 2.29. Found: C, 22.38; H, 3.77; N, 1.95.

$TBA_5H[P_2W_{15}V_3O_{62}(C_{20}H_{17}N_4O)RuCl_3]$, **5**. An 8-in. 5 mm NMR tube was charged with **4** (0.020 g, 3.8 µmol) and $RuCl_3(iPrSPh)_2(CH_3OH)$ (0.002 g, 3.8 µmol), and 0.4 mL of CD_3CN was added. The resulting clear dark orange solution was heated in the dark at 75−80 °C, and the progress of the complexation was monitored by NMR (^1H, ^{13}C and ^{31}P) every hour. After 4 h of heating, the solution color had changed to dark red and the reaction was stopped (full complexation as evidenced by ^{31}P and ^1H NMR). The red solution was poured into Et_2O (50 mL) to give a red precipitate, which was collected by centrifugation and washed with Et_2O (2 × 25 mL). Drying under vacuum gave **5** as a red solid (0.021 g, 96%). ^1H NMR (CD_3CN, 400 MHz, 298 K): δ −0.4 (br, 1H, $H_{3'}$), −5.2 (br, 1H, $H_{3/4/5}$), −6.8 (br, 1H, $H_{3/4/5}$), −8.9 (br, 1H, $H_{3/4/5}$), −36.7 (br, 1H, H_6). $^{13}C\{^1H\}$ NMR (CD_3CN, 100 MHz, 298 K): δ 131.49, 129.37, 126.96, 58.92, 23.96, 22.77, 19.91, 13.47 (peaks are missing because of the paramagnetism of the species). NMR assignment of the paramagnetic signals for **5** was done following previous studies on similar systems.[23] IR (KBr pellet, cm^{-1}): 2960 (v C−H, s), 2873 (v C−H, s), 1630 (v C=O, m), 1471 (v C−H, s), 1482 (v C−H, m), 1087 (v C−O, s), 950 (v V=O, vs), 911 (v W=O, vs), 817 (v M-O-M, vs),
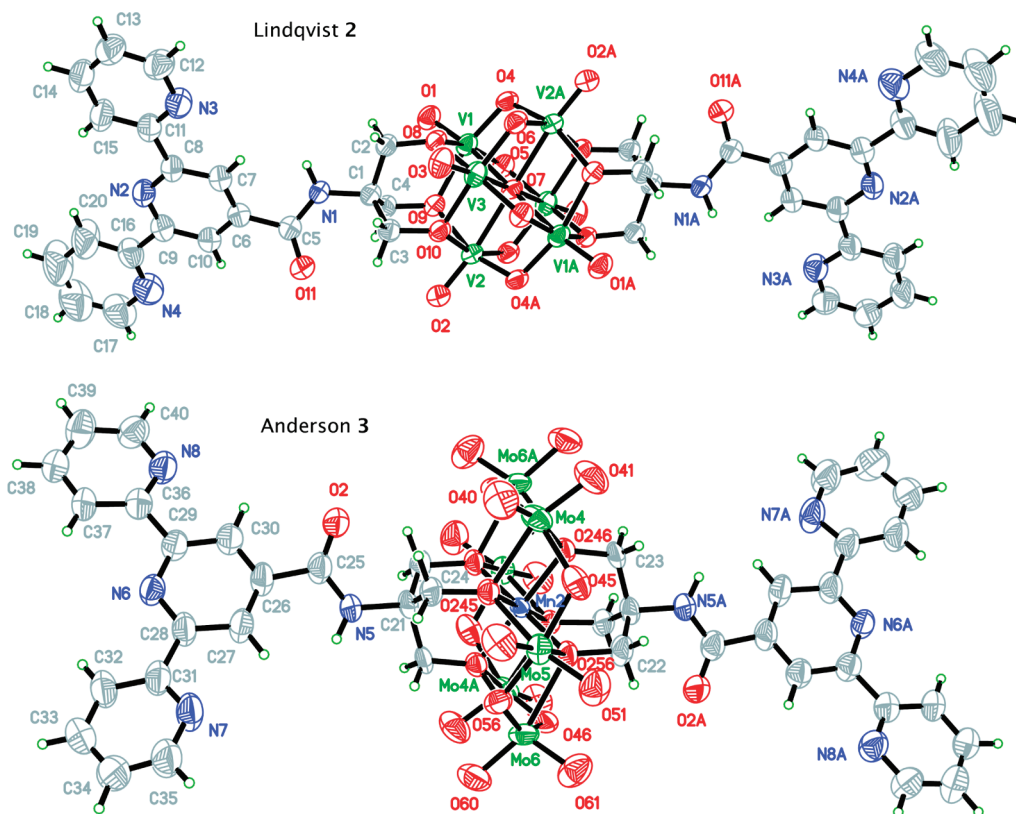
Figure 2. ORTEP diagram of Lindqvist **2** (top) and Anderson **3** (bottom) (thermal ellipsoids are drawn at 50% probability). Counterions and solvents were omitted for clarity.

736 (ν M-O-M, vs), 520 (m). UV–vis: λ /nm (ε /10^3 mol^{-1}·L·cm^{-1}) in CH$_3$CN, 271 (76.4), 281 (69.8), 307 (49.8), 400 (10.6), 491 (3.0). Anal. Calcd for (C$_{16}$H$_{36}$N)$_{5.5}$H$_{0.5}$[P$_2$W$_{15}$V$_3$O$_{62}$(C$_{20}$H$_{17}$N$_4$ORuCl$_3$)]: C, 22.23; H, 3.72; N, 2.28. Found: C, 22.74; H, 3.34; N, 2.63.

(C$_{16}$H$_{36}$N)[MnMo$_6$O$_{24}$(C$_{20}$H$_{17}$N$_4$OPdCl)$_2$], **6**. (C$_{16}$H$_{36}$N)$_3$[MnMo$_6$-O$_{26}$C$_{40}$H$_{34}$N$_8$] **3** (0.100 g, 0.04 mmol) and PdCl$_2$(CH$_3$CN)$_2$ (0.014 g, 0.05 mmol) were suspended in dry DMAc:CH$_3$CN 1:1 (1 mL). The mixture was heated at 80 °C for 6 h. The pale precipitate was centrifuged and washed with acetone (solid is slightly soluble in CH$_3$CN), then Et$_2$O, before being dried under vacuum to afford **6** (0.042 g, 46%). ^{1}H NMR (d$_6$-DMSO, 400 MHz, 298 K): δ 64 (br, 12H, H_b), 8.80 (m, 8H, $H_{3+3'}$), 8.75 (m, 4H, H_6), 8.49 (m, 4H, H_4), 7.90 (m, 4H, H_5), 3.16 (m, 8H, -NCH$_2$-), 1.56 (m, 8H, -NCH$_2$CH$_2$-), 1.30 (q, J = 10 Hz, 8H, -NCH$_2$CH$_2$CH$_2$-), 0.93 (t, J = 8 Hz, 12H, -NCH$_2$CH$_2$CH$_2$CH$_3$). Peaks in DMSO at r.t. in the ^{1}H spectrum are broadened because of paramagnetic Mn(III). They are described as "m". IR (KBr pellet, cm^{-1}): 2959 (ν C–H, m), 2935 (ν C–H, m), 2871 (ν C–H, m), 1674 (s), 1630 (ν C=O, s), 1607 (s), 1557 (s), 1479 (δ C–H, s), 1394 (δ C–H, m), 1318 (m), 1282 (m), 1244 (w), 1164 (w), 1100 (ν C=O, m), 1081 (m), 1031 (ν C=O, s), 942 (ν Mo=O, vs), 919 (ν Mo=O, vs), 901 (ν Mo=O, s), 793 (m), 666 (ν Mo–O–Mo, vs), 566 (m). UV–vis: λ/nm (ε/10^3 mol^{-1} L cm^{-1}) in DMF, 284 (33.6), 340 (9.4), 355 (8.9), 374 (7.2). Anal. Calcd for (C$_{16}$H$_{36}$N)[MnMo$_6$O$_{26}$C$_{40}$H$_{34}$N$_8$Pd$_2$Cl$_2$]·2C$_4$H$_9$NO: C, 32.23; H, 3.72; N, 6.46. Found: C, 31.93; H, 3.93; N, 6.20 (presence of 2 equiv of DMAc confirmed by ^{1}H NMR).

■ RESULTS AND DISCUSSION

Synthesis and Structural Characterization. Terpyridine-functionalized POMs **2**−**4** (Figure 1) were synthesized in several steps by adapted literature procedures.[16a,17,20,24,25] The common

starting material was a tris-(hydroxymethyl)-functionalized ter-pyridine **1**, which was obtained from terpyridine-4′-carboxy ethylester (Scheme 2).[26a] The ester was obtained by the oxida-tion of 4′-furyl-2,2′:6′,2″-terpyridine[26b,c] followed by esterifica-tion with ethanol via the acyl chloride. The synthesis of functionalized POMs **2**−**4** as their TBA salts (TBA = tetra-butylammonium) is always performed in dimethylacetamide (DMAc) to solubilize the terpyridyl ligand **1**. A first sign for the conservation of individual properties of organic ligands and inorganic POMs subsequent to the grafting is given by the comparison of the ^{1}H NMR spectra for **1**−**4**: the electronic influence of the cluster (paramagnetic for Anderson, or diamag-netic for Dawson and Lindqvist) on the chemical shifts is only seen up to the methylene protons of the ligand, the aromatic protons remaining unaffected (see Supporting Information, Figure 10). Further characterizations by ^{13}C NMR and IR spectroscopy, mass spectrometry, and elemental analysis were also consistent with, respectively, bis-functionalized Lindqvist and Anderson POMs **2** and **3** and with monofunctionalized Dawson POM **4**. Indeed, NMR spectroscopy allows characterization of the grafted organic moiety on each oxo-cluster, while IR spectroscopy confirms the POM structure by the observation of its character-istic bands. High-resolution mass spectrometry (HRMS) proves unambiguously the exact composition, which contains the cova-lent link between the organic and inorganic moieties.

For triol functionalized Lindqvist POMs cis and trans isomers are known,[27] while for Anderson structures δ and χ isomers exist.[25] Single crystals of TBA$_2$**2** (Lindqvist) and TBA$_3$**3**· C$_3$H$_7$NO·C$_4$H$_9$NO (Anderson, TBA = tetrabutylammonium) were obtained by diffusion of Et$_2$O into a DMF solution, and

Table 1. Details of X-ray Diffraction Studies for 2 and 3

	compound	
	2	3
formula	$[C_{16}H_{36}N]_2[C_{40}H_{34}N_8O_{21}V_6]$	$[C_{16}H_{36}N]_3[C_{40}H_{34}N_8O_{26}MnMo_6] \cdot C_3H_7NO \cdot C_4H_9NO$
M_w (g/mol); $F(000)$	1753.31; 3656	2560.92; 5280
T (K); wavelength (Å)	200; 1.54178	200; 0.71073
crystal system	monoclinic	monoclinic
space group	$C2/c$	$P21/n$
unit cell		
a (Å)	43.2834(12)	17.4447(18)
b (Å)	16.4677(5)	23.121(2)
c (Å)	16.4447(5)	28.984(3)
β (deg)	110.398(1)	106.268(2)
V (Å^3); Z; $d_{calcd.}$ (g/cm^3)	10986.4(6); 4; 1.060	11222(2); 4; 1.516
θ range (deg); completeness	2.90 to 72.75; 0.991	1.15 to 26.26; 1.000
collected reflections; R_σ	72898; 0.0261	283678; 0.0805
unique reflections; R_{int}	10854; 0.043	22654; 0.110
μ (mm^{-1}); abs. corr.	4.575; semiempirical from equivalents	0.833; semiempirical from equivalents
$R_1(F)$; $wR(F^2)$ $[I > 2\sigma(I)]$	0.0529; 0.1535	0.0661; 0.1926
$R_1(F)$; $wR(F^2)$ (all data)	0.0610; 0.1580	0.1040; 0.2134
GoF(F^2)	1.025	0.991
residual electron density (e$^-$/Å^3)	1.022 and −0.523	3.781 and −1.337

slow evaporation of a DMAc solution, respectively. Their molecular structures were determined by single crystal X-ray diffraction (Figure 2, Table 1). The trans isomer for the Lindqvist and the *δ* isomer for the Anderson POM (i.e., both alkoxo ligands are directly bonded to the Mn(III) center) were thus confirmed. Both anions rest on an inversion center in the crystal. In the Lindqvist compound, the asymmetric unit is constituted of half an anion and one TBA counterion. Two half anions, three TBA cations, and some solvent molecules are present in the asymmetric unit of the Anderson compound. The geometric features of the polyoxometalates are similar to those previously reported for related structures.[17−20,25] The distances between the two terpyridyl coordination sites are 21 Å, in **2**, and 19 Å, in **3**, with respective angles of 180° (inversion center) and 177.4° (angle measured between the nitrogen atoms of the central pyridine ring of each tpy and the central atom of each structure, the central oxygen of the Lindqvist and the manganese atom of the Anderson). In both structures, the nitrogens of the terpyridine moieties display a trans conformation about the interannular bond, as usual for such ligands.[28] As expected, there is no apparent steric hindrance from the POM to prevent the free rotation of the pyridyls and further coordination of metal cations. Thus, rigid grafting of the organic moiety maintains a defined spatial arrangement of subunits, which is appealing for the assembly of multicomponent covalent systems.

In the crystal, Lindqvist **2** arranges into chains through π-stacking of the terpyridine ligands (see Supporting Information, Figure 9). The lateral pyridine rings of two neighboring molecules are coplanar and 3.8 Å apart. In the crystal of the Anderson compound, no such stacking is observed, which indicates how difficult it is to predict the supramolecular arrangements of functionalized POMs in the solid state.

Electrochemical Characterization. The electrochemical data for the ligand and complexes **2**−**4** are gathered in Table 2.

Table 2. Redox Potentials for Model Ligand 1·tBu and for Grafted POMs 2−4^a

compound	redox potentials in V vs SCE.					
1·tBu^b	−1.94 (irr)					
2 Lindqvist	−1.97 (irr)	−1.87 (irr)	−0.52 (irr)			
3 Anderson	−1.92 (irr)	−1.28 (irr)	0.75 (rev)			
4^c Dawson	−1.96	−1.61	−1.16	−1.05	−0.82	0.08

^{a} Redox potentials (Volts) are measured at r.t. and vs SCE for degassed DMF solutions with 1 mM of compound (0.1 M TBAPF$_6$). Glassy carbon electrode and ferrocene as internal standard ($E = +0.39$ V vs SCE in CH$_3$CN and $E = +0.43$ V vs SCE in DMF) were used. For irreversible processes, the potential is given for the cathodic wave; for reversible processes, the half-wave potential is given. ^{b} Measurement performed in degassed CH$_3$CN, because of the increased problems of adsorption of multicharged species in DMF. ^{c} Process determined by DPV because of ill-defined waves in CV.

The redox behavior of the ligand **1·tBu**, for which the triol function has been substituted by a *tert*-butyl group, has been determined for comparison to that of the organic moiety grafted on the oxo framework of the POM. It shows that the reduction around −2 V vs SCE observed in all compounds is ligand based.

Lindqvist structure **2** displays a reduction at −0.52 V vs SCE in agreement with analogous systems.[17] Depending on the experimental conditions, the process is more or less resolved; DMF is here a better solvent than CH$_3$CN for the solubility of species and for charge transfer. This process is assigned to the reduction of the vanadium centers.

Anderson derivative **3** exhibits one reversible oxidation attributed to Mn(III)/Mn(IV) (+0.75 V vs SCE). The broad wave at −1.28 V vs SCE is assigned to the Mn(III)/Mn(II)

reduction. Broadening of this process has been observed before on functionalized Anderson POMs.[29] The next reduction at −1.92 V is a superposition of Mo(VI) and a ligand reduction.

Dawson derivative **4** displays several processes on a wide range of potentials (+0.5 to −2.0 V vs SCE; Table 2). The reductions are centered on V(V), W(VI), and the organic ligand in order of decreasing potentials. The enlargement of the observed signals is not due to irreversibility of the processes, but to adsorption of the compound on the surface of the glassy carbon electrode.

The comparison of the redox behaviors of hybrids **2**−**4** and the model free ligand **1·tBu** demonstrates that the influence of the cluster on the redox properties of the ligand is negligible. The subunits are electronically isolated in the ground-state: the POM subunits maintain their functionality as an electron reservoir despite the grafting of the organic moiety, with several processes in an accessible redox range.
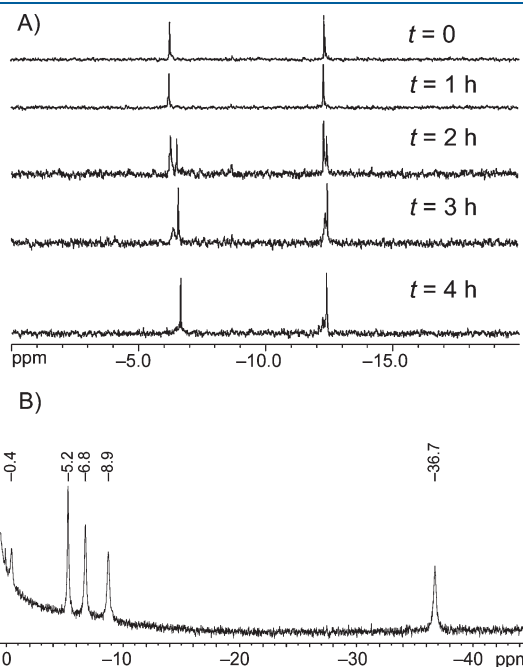
Electronic Absorption Spectroscopy. UV−visible absorption data are reported in Table 3. The grafted POM structures are orange (Anderson and Lindqvist) to yellow (Dawson), because of the trailing end of the LMCT O → M absorption in the lower energy UV region. Model ligand **1·tBu** presents four bands between 210 and 310 nm, due to $\pi \rightarrow \pi^*$ transitions. By comparison with this spectrum, it can be concluded that for the Lindqvist derivative **2**, all transitions distinguished between 230 and 310 nm are ligand-centered, while the longer wavelength band at 350 nm is due to O → V LMCT transitions. For the Anderson

derivative **3**, intense O → Mo LMCT and ligand-centered $\pi \rightarrow \pi^*$ transitions are superimposed in the UV region. Bands can be distinguished at the absorption maxima of the ligand, but the ε values indicate a contribution from the POM. Similarly, for Dawson derivative **4**, the intense O → M LMCT transitions (M = W[30] and V[31]) cover the $\pi \rightarrow \pi^*$ transitions from the terpyridine ligand. Within the hybrid **2**−**4** POM series, the $\pi \rightarrow \pi^*$ transitions remain quite unchanged compared to the model ligand **1·tBu**. Thus, the UV−visible absorption data confirm the electronic isolation between the subunits, POM, and organic ligand, in agreement with the observations by ^{1}H NMR and electrochemistry.

Figure 3. (A) ^{31}P NMR monitoring of the formation of **5** in CD$_3$CN at reflux. (B) ^{1}H NMR after 4 h (for full monitoring, see Supporting Information). The reaction is completed after 4 h, and the obtained species displays characteristic peaks for a Dawson phosphovanadotungstate and a [Ru(4′-Rtpy)Cl$_3$] coordination motif.

Table 3. UV-visible Electronic Absorption Measured in CH$_3$CN at r.t. for the Ligand 1·tBu and for Functionalized POMs 2−4[a]
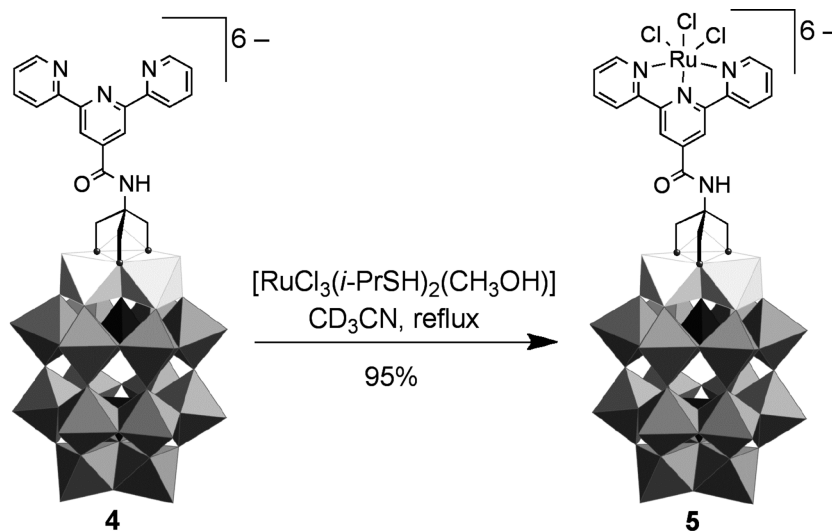
compound	absorption, λ/nm, ($\varepsilon/10^3$ mol^{-1}·cm^{-1}·L)		
1·tBu	237 (24.0)	278 (20.5)	310 (10.1)
	250 (sh)		
2	233 (61.1)	276 (55.0)	310 (26.7);
	248 (57)		350 (7.88.)
3	233 (148)	274 (88.5)	312 (36.6)
	250 (124)		
4	250 (71.9)	271 (69.9)	307 (38.0)

[a] sh = shoulder.

Scheme 3. Formation of a Ru-Complex on POM 5

Scheme 4. Reaction Conditions for the Formation of 6

Figure 4. Comparison of ^{1}H NMR spectra (400 MHz, d_6-DMSO) of POM **3** and **6** showing the complexation of the {PdCl}$^+$ moiety.
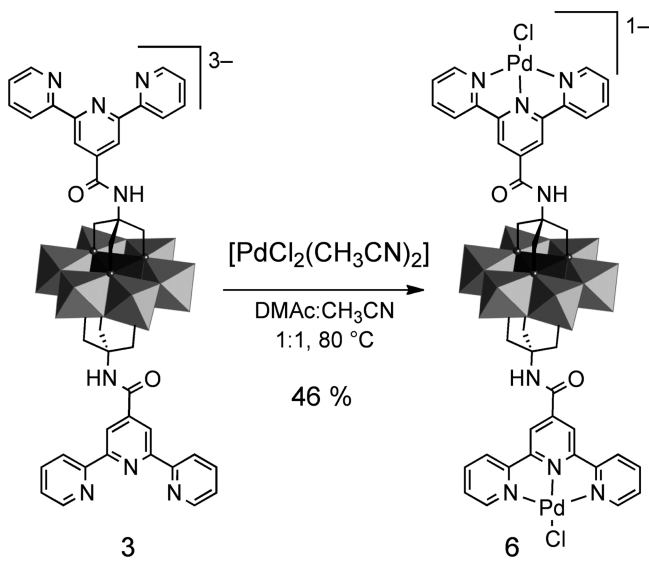
Metal Complexation. With the POM-grafted ligands in hand, we investigated the complexation of Pd(II) starting from PdCl$_2$-(CH$_3$CN)$_2$ and Ru(III) starting from RuCl$_3$·H$_2$O and RuCl$_3$-(*i*PrSPh)$_2$(CH$_3$OH), respectively.[32] We report herein our results with POMs **3** and **4**.

Following typical Ru-polypyridine complexation conditions, we studied the complexation of the neutral moiety {RuCl$_3$} with **4**. Indeed the hybrid [Cl$_3$Ru(**4**)]$^{6-}$ (**5**, Scheme 3) would be an appealing intermediate for the synthesis of heteroleptically coordinated hybrids. We first tried the classical Ru(III) precursor RuCl$_3$·H$_2$O. In CH$_3$CN, after 15 min at reflux, we could observe a complicated mixture of products by ^{31}P NMR, but the formation of the desired terpyridine complex was ascertained by UV–visible spectroscopy. The new transitions observed at 390 and 490 nm were assigned, respectively, to LMCT Cl → Ru and MLCT Ru → (tpy), in agreement with Chatt's observations[32] and by comparison to the reference complex [(Br-ph-tpy)-RuCl$_3$].[23] However, the desired product could not be isolated pure. As we recently reported the coordination of [RuCl$_3$-(*i*PrSPh)$_2$(CH$_3$OH)] with tridentate polypyridine ligands and the monitoring of the reaction by ^{1}H NMR, despite the paramagnetism of the Ru center,[23] we decided to investigate its reaction with **4**. In the ^{1}H NMR spectra, the aromatic signals of the POM derivative disappeared progressively, with the simultaneous appearance of the characteristic peaks of the {(R-tpy)-Ru^{III}Cl$_3$} coordination motif at −0.4/−5.2/−6.8/−8.9/−36.7 ppm (see Figure 3B and Supporting Information, Figure 11). The signals of the thioether ligands, whose integration with respect to the POM remains unchanged throughout the reaction, served as internal reference. All the chemical shifts fall well into the range expected for a [Ru(tpy)Cl$_3$]-type complex. Assignment of the signals to protons of the tpy-moiety is difficult, because the paramagnetism masks the ^{1}H–^{1}H coupling interactions. In accordance with previous work,[41] the signal at −36.7 ppm can be safely attributed to H-6, closest to Ru^{III}. The less shielded signal at −0.4 ppm corresponds likely to the most remote H-3′. The remaining three signals correspond to H-3, H-4, and H-5. As no other highly shielded signals appear, only one paramagnetic complex is present. In the ^{31}P NMR spectra, a new Dawson

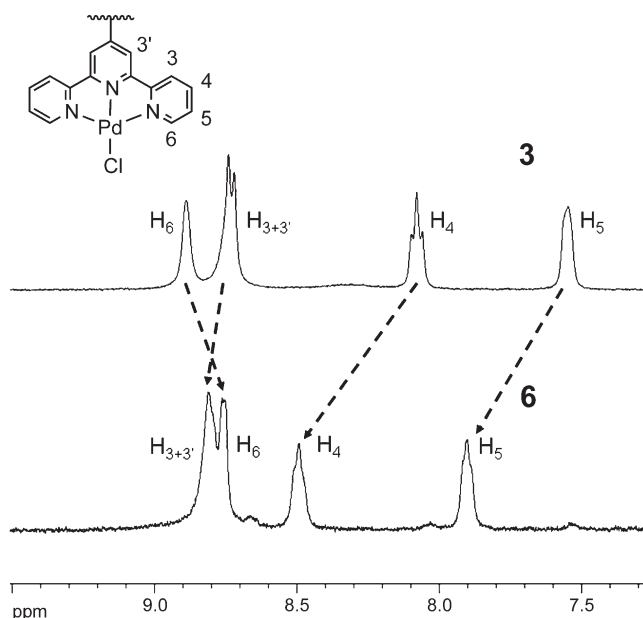species is formed increasingly over time and remains stable after 4 h reflux in CH$_3$CN. From both ^{13}C and ^{31}P NMR spectra, it is clear that there is neither important loss of functionalization nor degradation of the POM within 4 h.

Hybrid **5** could be isolated as the TBA salt by precipitation in Et$_2$O, and was further characterized. Electrospray mass spectrometry gave signals for intact POM **5** associated with different counterions (TBA$^+$ or H$^+$) and fragments that result from the loss of chloride ligands (see Supporting Information, Figure 6 and table). This indicates clearly the composition and consequently the covalent link within the hybrid POM. IR spectroscopy confirmed further the integrity of the POM framework, as all characteristic metal-oxo vibrational bands in the domain 600–1100 cm^{-1} for the functionalized Dawson ion are conserved (see Supporting Information, Figure 21). UV–vis spectroscopy (in Supporting Information, Figure 14) showed that the introduction of the Ru^{III} chromophore draws the absorption of **5** into the visible, with a red compound (instead of the yellow starting material **4**, in Supporting Information, Figure 13). Two absorption bands, one at 491 nm and the other at 400 nm, are in accordance with the transitions expected for a Ru^{III} coordinated to a tpy ligand and three chlorides.[32]

^{1}H NMR and UV–vis spectroscopies support the assignment of a [Ru(tpy)Cl$_3$]-type complex, ^{31}P and IR show the intact Dawson POM, and MS proves the covalent link between both moieties. Thus, the combined analytical data prove unambiguously the successful coordination of Ru^{III} to the POM grafted terpyridine ligand, thus demonstrating our modular strategy as outlined in Scheme 1.

As a second example, we investigated the complexation of Pd^{II} ion. On the basis of the preferential square-planar geometry of this d^8 metal, and the multiple denticity of the terpyridine ligand, any competitive oligomerization or polymerization should be prevented (often observed for analogous mono- and bidentate ligands).[20]

Two equivalents of [PdCl$_2$(CH$_3$CN)$_2$] were reacted with **3** in DMAc to yield the bis-palladium species **6** quantitatively (Scheme 4). Surprisingly, the yield is also quantitative in the

formation of **6** with only 1 equiv of Pd(II), leaving unreacted POM **3** in solution. The driving force of this complexation lies in the difference of solubility as **6** precipitates in the reaction media. It is interesting to note that the complexation of a metal on a functionalized POM can be optimized by playing with the solubility, to maximize the complexation thus facilitating the purification process.

The complexation of a Pd^{II} on each terpyridyl site is confirmed by ^{1}H NMR spectroscopy (Figure 4) as the number of signals indicates a symmetric compound with two equivalent ligands. The chemical shift variations between **3** and **6** correspond to the signature of coordinated terpyridine as δ values compare very well with those reported for $[Pd(tpy)Cl]^+$ type complexes (assignment in Figure 4).[33] UV−vis absorption spectroscopy shows two bands in the near UV region (355 and 374 nm) that are also consistent with $[Pd(tpy)Cl]^+$ coordination. The model complex $[Pd(4'-BrC_6H_4-tpy)Cl]^+$ (**7**) further confirms the NMR and UV−vis signature (see Supporting Information). The characteristic signature in IR spectroscopy for the Anderson POM is unchanged between **3** and **6** (see Supporting Information, Figure 20). In ESI-MS, the signal at m/z 1966.24 confirms the composition of **6**. Once again, the combined analytical data prove unambiguously the nature of this compound.

■ CONCLUSIONS

In conclusion, we have synthesized unique POM clusters functionalized with terpyridine ligands to introduce tridentate binding sites available for metal complexation on the POM. Our modular strategy allows the same ligand to be incorporated into diverse POM frameworks. We have also demonstrated the successful coordination of the hybrid organic−inorganic POM ligands to transition metal ions. As proof of principle, {RuCl$_3$} was bound to the terpyridine of Dawson **4**, and {PdCl}$^+$ was bound to both terpyridines of Anderson **3**. The obtained complexes were fully characterized by multiple spectroscopic techniques to prove the intact POM framework and binding to the grafted organic ligand. Further coordination chemistry of POMs **2**−**4**, together with electrochemical studies on these hybrid compounds, will be reported in due course.

We have shown here that the triol motif is a useful function to graft terpyridines onto three different POMs. We[16a,19,20] and others[17] reported the same approach for pyridines and porphyrins. We have also prepared the corresponding bipyridine derivatives.[34] Therefore, this approach corresponds to a modular strategy to access discrete transition metal functionalized POMs.

The conservation of the intrinsic properties of the subunits in larger assemblies allows better control of the intramolecular processes, especially regarding *directionality* of the processes, which is of crucial importance in large arrays. Moreover, hybrid **5** opens up a way for heteroleptically coordinated hybrids, which may present enhanced photophysical properties compared to homoleptic analogues.[35] On the other hand, **6** is a linear metalated building-block, which could prove useful in the build up of larger POM-based supramolecular assemblies. We now focus our efforts on achieving a new degree of versatility in this metal-directed self-assembly strategy.

■ ASSOCIATED CONTENT

Ⓢ Supporting Information. Crystallographic data in CIF format. Further details (Figures 1−21) as noted in the text.

This material is available free of charge via the Internet at http://pubs.acs.org.

■ AUTHOR INFORMATION

Corresponding Author

*E-mail: garry.hanan@umontreal.ca (G.S.H); bernold.hasenknopf@upmc.fr (B.H.).

■ ACKNOWLEDGMENT

■ REFERENCES

(1) (a) Descalzo, A.; Martinez-Manez, R.; Sancenon, F.; Hoffmann, K.; Rurack, K. *Angew. Chem., Int. Ed.* **2006**, *45*, 5924–5948. (b) Wang, M.; Xu, G.; Zhang, Z.; Guo, G. *Chem. Commun.* **2010**, *46*, 361–379. (c) Sanchez, C.; Julian, B.; Belleville, P.; Popall, M. *J. Mater. Chem.* **2005**, *15*, 3559–3592. (d) Kitagawa, S.; Kitaura, R.; Noro, S. *Angew. Chem., Int. Ed.* **2004**, *43*, 2334–2375. (e) Horiuchi, S.; Tokura, Y. *Nat. Mater.* **2008**, *7*, 357–366. (f) Hong, M. *Cryst. Growth Des.* **2007**, *7*, 10–14. (g) Fukuzumi, S.; Kojima, T. *J. Mater. Chem.* **2008**, *18*, 1427–1439.

(2) (a) *Polyoxometalate Molecular Science*; Borras-Almenar, J. J., Coronado, E., Müller, A., Pope, M. T., Eds.; Kluwer Academic Publishers: Dordrecht, The Netherlands, 2003; Vol. 98. (b) Long, D. L.; Burkholder, E.; Cronin, L. *Chem. Soc. Rev.* **2007**, *36*, 105–121. (c) Long, D.-L.; Tsunashima, R.; Cronin, L. *Angew. Chem., Int. Ed.* **2010**, *49*, 1736–1758.

(3) (a) Odobel, F.; Séverac, M.; Pellegrin, Y.; Blart, E.; Fosse, C.; Cannizzo, C.; Mayer, C.; Elliott, K; Harriman., A. *Chem.—Eur. J.* **2009**, *15*, 3130–3138. (b) Harriman, A.; Elliott, K.; Alamiry, M.; Le Pleux, L.; Séverac, M.; Pellegrin, Y.; Blart, E.; Fosse, C.; Cannizzo, C.; Mayer, C.; Odobel, F. *J. Phys. Chem. C* **2009**, *113*, 5834–5842. (c) Elliott, K.; Harriman, A.; Le Pleux, L.; Pellegrin, Y.; Blart, E.; Mayer, C.; Odobel, F. *Chem. Phys. Phys. Chem.* **2009**, *11*, 8767–8773.

(4) (a) AlDamen, M. A.; Cardona-Serra, S.; Clemente-Juan, J. M.; Coronado, E.; Gaita-Arino, A.; Marti-Gastaldo, C.; Luis, F.; Montero, O. *Inorg. Chem.* **2009**, *48*, 3467–3479. (b) Charron, G.; Giusti, A.; Mazerat, S.; Mialane, P.; Gloter, A.; Miserque, F.; Keita, B.; Nadjo, L.; Filoramo, A.; Riviere, E.; Wernsdorfer, W.; Huc, V.; Bourgoin, J.-P.; Mallah, T. *Nanoscale* **2010**, *2*, 139–144. (c) Ritchie, C.; Ferguson, A.; Nojiri, H.; Miras, H. N.; Song, Y.-F.; Long, D.-L.; Burholder, E.; Murrie, M.; Kögerler, P.; Brechin, E. K.; Cronin, L. *Angew. Chem., Int. Ed.* **2008**, *47*, 5609–5612.

(5) (a) Ito, T.; Yashiro, H.; Yamase, T. *Langmuir* **2006**, *22*, 2806–2810. (b) Compain, J.-D.; Deniard, P.; Dessapt, R.; Dolbecq, A.; Oms, O.; Secheresse, F.; Marrot, J.; Mialane, P. *Chem. Commun.* **2010**, *46*, 7733–7735. (c) de Oliveira, M.; Lopes de Souza, A.; Schneider, J.; Rodrigues-Filho, U. P. *Chem. Mater.* **2011**, *23*, 953–963. (d) Liu, S.; Möhwald, H.; Volkmer, D.; Kurth, D. G. *Langmuir* **2006**, *22*, 1949–1951.

(6) (a) Coronado, E.; Gimenez-Saiz, C.; Gomez-Garcia, C. *Coord. Chem. Rev.* **2005**, *249*, 1776–1796. (b) Coronado, E.; Curreli, S.; Gimenez-Saiz, C.; Gomez-Garcia, C. J.; Alberola, A.; Canadell, E. *Inorg. Chem.* **2009**, *48*, 11314–11324. (c) Coronado, E.; Gimenez-Saiz, C.;

Gomez-Garcia, C. J.; Capelli, S. C. *Angew. Chem., Int. Ed.* **2004**, *43*, 3022–3025.

(7) (a) Das, S. K. *Supramolecular Structures and Polyoxometalates, in Macromolecules Containing Metal and Metal-Like Elements: Supramolecular and Self-Assembled Metal-Containing Materials*; A. S. Abd-El Aziz, Carraher, C. E., Pittman, C. U.; , Zeldin, M., Eds.; John Wiley & Sons, Inc.: Hoboken, NJ, 2009; Vol. 9. (b) Liu, H.; Gomez-Garcia, C. J.; Peng, J.; Sha, J.; Li, Y.; Yan, Y. *Dalton Trans.* **2008**, 6211–6218. (c) Schaming, D.; Costa-Coquelard, C.; Lampre, I.; Sorgues, S.; Erard, M.; Liu, X.; Liu, J.; Sun, L.; Canny, J.; Thouvenot, R.; Ruhlmann, L. *Inorg. Chim. Acta* **2010**, *363*, 2185–2192. (d) Yao, C.; Yan, L.-K.; Guan, W.; Liu, C.-G.; Song, P.; Su, Z.-M. *Dalton Trans.* **2010**, *39*, 7645–7649. (e) Yokoyama, A.; Kojima, T.; Ohkubo, K.; Shiro, M.; Fukuzumi, S. *J. Phys. Chem. A* **2011**, *115*, 986–997. (f) Belai, N.; Pope, M. T. *Chem. Commun.* **2005**, 5760. (g) Berardi, S.; Carraro, M.; Iglesias, M.; Sartorel, A.; Scorrano, G.; Albrecht, M.; Bonchio, M. *Chem.—Eur. J.* **2010**, *16*, 10662–10666.

(8) (a) Papaconstantinou, E. *Chem. Soc. Rev.* **1989**, *18*, 1. (b) Yamase, T. *Catal. Surv. Asia* **2003**, *7* (4), 203. (c) Puntoriero, F.; La Ganga, G.; Sartorel, A.; Carraro, M.; Scorrano, G.; Bonchio, M.; Campagna, S. *Chem. Commun.* **2010**, *46*, 4725–4727. (d) Toma, F. M.; Sartorel, A.; Iurlo, M.; Carraro, M.; Parisse, P.; Maccato, C.; Rapino, S.; Gonzalez, B. R.; Amenitsch, H.; Da Ros, T.; Casalis, L.; Goldoni, A.; Marcaccio, M.; Scorrano, G.; Scoles, G.; Paolucci, F.; Prato, M.; Bonchio, M. *Nat. Chem.* **2010**, *2*, 826–831.

(9) (a) Keyes, T.; Gicquel, E.; Guerin, L.; Forster, R.; Hultgren, V.; Bond, A.; Wedd, A. *Inorg. Chem.* **2003**, *42*, 7897. (b) Seery, M.; Guerin, L.; Forster, R.; Gicquel, E.; Hultgren, V.; Bond, A.; Wedd, A.; Keyes, T. *J. Phys. Chem. A* **2004**, *108*, 7399. (c) Fay, N.; Hultgren, V.; Wedd, A.; Keyes, T.; Forster, R.; Leane, D.; Bond, A. *Dalton Trans.* **2006**, 4218.

(10) Darwent, J. R.; Douglas, P.; Harriman, A.; Porter, G.; Richoux, M.-C. *Coord. Chem. Rev.* **1982**, *44*, 83–126.

(11) (a) Krasna, A. *Photochem. Photobiol.* **1979**, *29*, 267. (b) Harriman, A. *J. Photochem.* **1984**, *25*, 33.

(12) (a) Lan, Y.-Q.; Li, S.-L.; Shao, K.-Z.; Wang, X.-L.; Su, Z.-M. *Dalton Trans.* **2008**, 3824–3835. (b) Pradeep, C. P.; Long, D.-L.; Cronin, L. *Dalton Trans.* **2010**, *39*, 9443–9457.

(13) (a) Proust, A.; Thouvenot, R.; Gouzerh, P. *Chem. Commun.* **2008**, 1837–1852. (b) Dolbecq, A.; Dumas, E.; Mayer, C. R.; Mialane, P. *Chem. Rev.* **2010**, *110*, 6009–6048.

(14) (a) Bareyt, S.; Piligkos, S.; Hasenknopf, B.; Gouzerh, P.; Lacote, E.; Thorimbert, S.; Malacria, M. *J. Am. Chem. Soc.* **2005**, *127*, 6788–6794. (b) Micoine, K.; Hasenknopf, B.; Thorimbert, S.; Lacôte, E.; Malacria, M. *Org. Lett.* **2007**, *9*, 3981–3984. (c) Joo, N.; Renaudineau, S.; Delapierre, G.; Bidan, G.; Chamoreau, L.-M.; Thouvenot, R.; Gouzerh, P.; Proust, A. *Chem.—Eur. J.* **2010**, *16*, 5043. (d) Matt, B.; Renaudineau, S.; Chamoreau, L.-M.; Afonso, C.; Izzet, G.; Proust, A. *J. Org. Chem.* **2011**, *76*, 3107–3112.

(15) (a) Xu, B.; Peng, Z.; Wei, Y.; Powell, D. *Chem. Commun.* **2003**, 2562. (b) Kang, J.; Xu, B.; Peng, Z.; Zhu, X.; Wei, Y.; Powell, D. R. *Angew. Chem., Int. Ed.* **2005**, *44*, 6902.

(16) (a) Allain, C.; Favette, S.; Chamoreau, L.-M.; Vaissermann, J.; Ruhlmann, L.; Hasenknopf, B. *Eur. J. Inorg. Chem.* **2008**, 3433–3441. (b) Villanneau, R.; Racimor, D.; Messner-Henning, E.; Rousselière, H.; Picart, S.; Thouvenot, R.; Proust, A. *Inorg. Chem.* **2011**, *50*, 1164–1166.

(17) Han, J. W.; Hardcastle, K. I.; Hill, C. L. *Eur. J. Inorg. Chem.* **2006**, 2598–2603.

(18) (a) Janjua, M. R. S. A.; Guan, W.; Yan, L.; Su, Z.-M.; Ali, M.; Bukhari, I. H. *J. Mol. Graphics Modell.* **2010**, *28*, 735–745. (b) Stark, J.; Young, V.; Maatta, E. *Angew. Chem., Int. Ed.* **1995**, *34*, 2547. (c) Xu, B. B.; Lu, M.; Kang, J. H.; Wang, D.; Brown, J.; Peng, Z. H. *Chem. Mater.* **2005**, *17*, 2841.

(19) Marcoux, P.; Hasenknopf, B.; Vaissermann, J.; Gouzerh, P. *Eur. J. Inorg. Chem.* **2003**, 2406.

(20) Favette, S.; Hasenknopf, B.; Vaissermann, J.; Gouzerh, P.; Roux, C. *Chem. Commun.* **2003**, 2664–2665.

(21) Duffort, V.; Thouvenot, R.; Afonso, C.; Izzet, G.; Proust, A. *Chem. Commun.* **2009**, 6062–6064.

(22) (a) Bar-Nahum, I.; Neumann, R. *Chem. Commun.* **2003**, 2690–2691. (b) Bar-Nahum, I.; Cohen, H.; Neumann, R. *Inorg. Chem.* **2003**, *42*, 3677–3684.

(23) Santoni, M.-P.; Pal, A.; Hanan, G. S.; Proust, A.; Hasenknopf, B. *Inorg. Chem. Commun.* **2011**, *14*, 399.

(24) Hou, Y.; Hill, C. *J. Am. Chem. Soc.* **1993**, *115*, 11823.

(25) Hasenknopf, B.; Delmont, R.; Herson, P.; Gouzerh, P. *Eur. J. Inorg. Chem.* **2002**, 1081–1087.

(26) (a) Husson, J.; Beley, M.; Kirsch, G. *Tetrahedron Lett.* **2003**, *44*, 1767. (b) Cooke, M.; Tremblay, P. M.; Hanan, G. S. *Inorg. Chem. Commun.* **2007**, *10*, 1365. (c) Newkome, G.; Baker, G. R.; Arai, S.; Saunders, M. J.; Russo, P. S.; Theriot, K. J.; Moorefield, C. N.; Rogers, L. E.; Miller, J. E.; Lieux, T. R.; Murray, M. E.; Phillips, B.; Pascal, L. *J. Am. Chem. Soc.* **1990**, *112*, 8458.

(27) (a) Chen, Q.; Goshorn, D.; Scholes, C.; Tan, X.; Zubieta, J. *J. Am. Chem. Soc.* **1992**, *114*, 4667. (b) Chen, Q.; Zubieta, J. *Inorg. Chem.* **1990**, *29*, 1456–1458. (c) Müller, A.; Meyer, J.; Bôgge, H.; Stammler, A.; Botar, A. *Z. Anorg. Allg. Chem.* **1995**, *621*, 1818.

(28) Hanan, G. S.; Schubert, U. S.; Volkmer, D.; Rivière, E.; Lehn, J.-M.; Kyritsakas, N.; Fisher, J. *Can. J. Chem.* **1997**, *75*, 169.

(29) Schaming, D.; Allain, C.; Farha, R.; Goldmann, M.; Lobstein, S.; Giraudeau, A.; Hasenknopf, B.; Ruhlmann, L. *Langmuir* **2010**, *26*, 5101–5109.

(30) Pope, M. T. *Heteropoly and Isopoly Oxometalates*; Springer: Berlin, Germany, 1983.

(31) Li, C.; Cao, R.; O'Halloran, K.; Ma, H.; Wu, L. *Electrochim. Acta* **2008**, *54*, 484.

(32) Chatt, J.; Leigh, G. J.; Storace, A. P. *J. Chem. Soc. (A)* **1971**, 1380–1389.

(33) Beves, J. E.; Constable, E. C.; Housecroft, C. E.; Neuburger, M.; Schaffner, S. *Inorg. Chem. Commun.* **2007**, *10*, 1185–1188.

(34) Santoni, M. P. Ph.D. Thesis , Université Pierre et Marie Curie, Paris, France, and Université de Montréal, Montréal, Canada, 2010.

(35) (a) Medlycott, E.; Hanan, G. *Chem. Soc. Rev.* **2005**, *34*, 133. (b) Medlycott, E.; Hanan, G. *Coord. Chem. Rev.* **2006**, *250*, 1763.